SCIENTIFIC REPORTS

OPEN

SUBJECT AREAS:
BIOTECHNOLOGY
DISEASES

Received
11 September 2014

Accepted
22 December 2014

Published
21 January 2015

Correspondence and requests for materials should be addressed to H.J. (hijung@yonsei.ac.kr)

A patchless dissolving microneedle delivery system enabling rapid and efficient transdermal drug delivery

Shayan F. Lahiji, Manita Dangol & Hyungil Jung

Department of Biotechnology, Yonsei University, 50 Yonsei-ro, Seodaemun-gu, Seoul, 120-749, Korea.

Dissolving microneedles (DMNs) are polymeric, microscopic needles that deliver encapsulated drugs in a minimally invasive manner. Currently, DMN arrays are superimposed onto patches that facilitate their insertion into skin. However, due to wide variations in skin elasticity and the amount of hair on the skin, the arrays fabricated on the patch are often not completely inserted and large amount of loaded materials are not delivered. Here, we report "Microlancer", a novel micropillar based system by which patients can self-administer DMNs and which would also be capable of achieving 97 ± 2% delivery efficiency of the loaded drugs regardless of skin type or the amount of hair on the skin in less than a second.

Among various possible delivery routes, drugs are most often administered either orally or by parenteral injection[1–3]. Although oral drug delivery is the most convenient and patient-friendly drug administration method, the bioavailability of numerous orally ingested drugs is greatly reduced due to first-pass elimination, which can be influenced by a number of physiological factors, such as serum protein levels, enzyme activity and gastrointestinal motility of the drug in the body[1,4]. Hypodermic injection is more expedient, and can circumvent the aforementioned effects by delivering drugs directly into the blood stream[5]. However, hypodermic injection also has some drawbacks, including the high level of expertise required to administer an injection, the trypanophobia of certain patients, and the occasional risk of infections acquired through needle sticks[6–8]. To mitigate these limitations, many researchers have developed microneedle (MN)-mediated drug delivery systems[5,9–11], which enable patients to painlessly self-administer therapeutic micro- and macromolecule drugs[12–16].

Dissolving microneedles (DMNs) are polymeric, microscopic needles that encapsulate pharmaceuticals within their matrix[1,17]. Insertion of DMNs into the skin catalyzes the degradation of the polymeric compound, thereby releasing the drug for systemic or local delivery[18,19]. Unlike hypodermic injections, DMNs are fully biocompatible and generate no biohazardous sharps waste[3,20]. Moreover, DMNs have also been shown to be more dose-effective compared with subcutaneous immunizations[21–23]. Currently, the only DMN application method used is to superimpose an array of microneedles onto patches that facilitates the insertion and maintenance of the microneedles. Although patches are widely used as supports in DMN applications, the efficacy of drug delivery that can be achieved with patches is often significantly reduced due to high variation in skin elasticity, which can result in incomplete insertion of the DMNs[17,24,25]. Furthermore, the chemicals used in the patch materials can cause skin irritation and/or allergic reactions; other disadvantages to patch delivery include difficulties in adhering to flexible body joint areas and to hairy skin. Moreover, patients must wait for extended periods of time for the DMNs to dissolve completely before the patch can be removed[26].

Recently, various approaches have been developed to overcome the limitations associated with DMN-mediated drug delivery. Two-layered DMNs and arrowhead DMNs, which consist of a therapeutic polymer layer and a shaft, respectively, have been developed to deliver drug-based polymer tips with greater efficiency[20,24,27]. Alternatively, a soft lithography approach based on a water soluble patch system has also been introduced to increase delivery efficacy by dissolving the patch after DMN application[28]. Although these approaches could improve the general delivery efficacy of DMNs, the fundamental problems associated with incomplete insertion of DMN patch systems have not been fully addressed yet. Needleless injection systems have been developed as patchless drug delivery systems to overcome the aforementioned limitations by injecting liquid drugs directly into the skin. In needle-less jet injection systems, the pressurized liquid drug passes through a microaperture and creates a narrow stream of high-speed fluid that penetrates the skin[29,30]. Although jet injector-based drug delivery systems are an effective drug delivery method, injection depth is difficult to control; moreover, the application of these injection systems is often associated with pain, irritation and patient discomfort. Furthermore, jet injector-

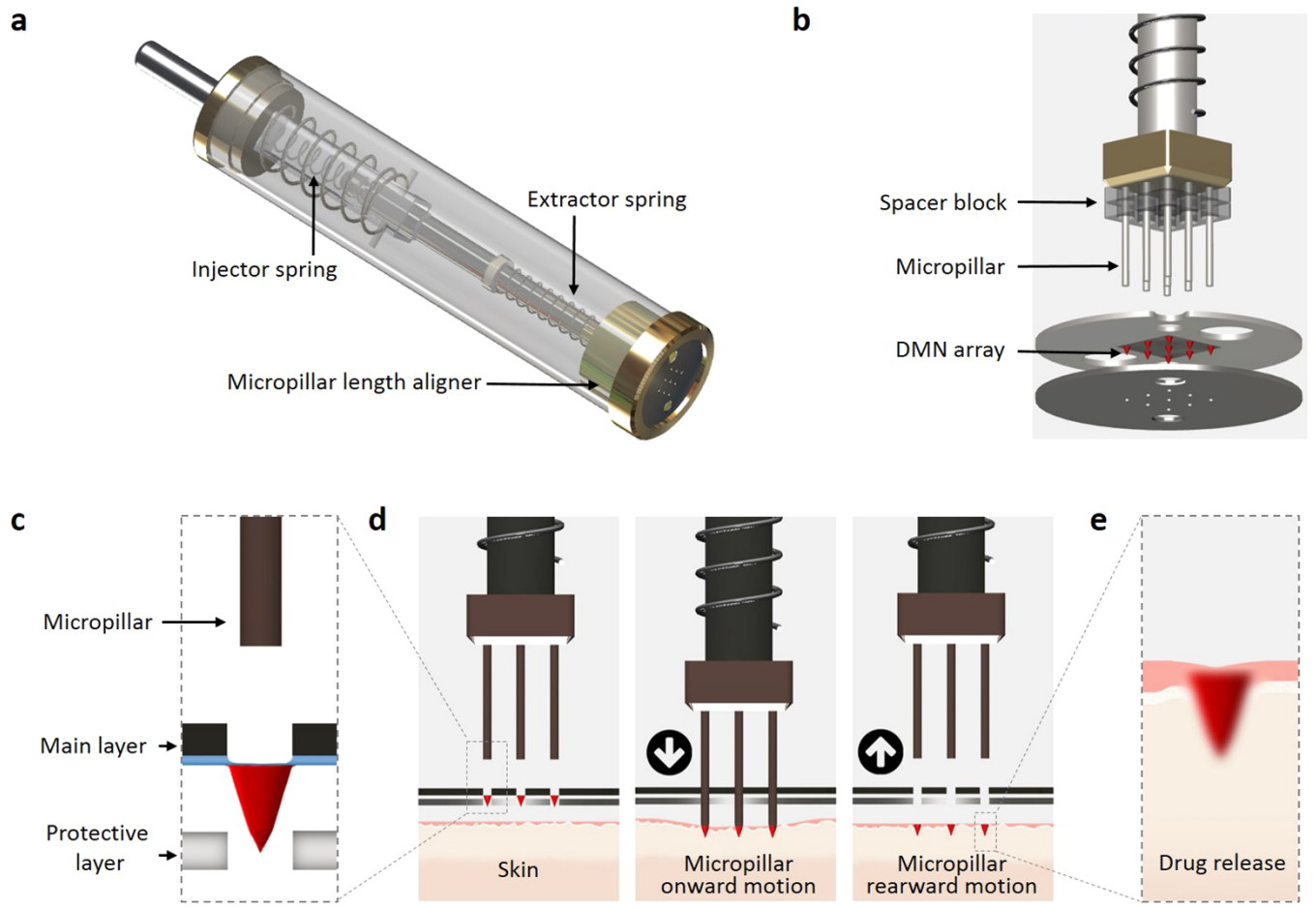

Figure 1 | Schematic illustration of the Microlancer and its performance. (a) Main units of Microlancer. (b) A 3 × 3 DMN array with respect to the other components of the Microlancer. (c) The positioning of the hole and its alignment with the micropillar results in the physical detachment of the DMNs. A protective layer ensures that only DMNs, and not the surrounding layer, are detached from the main layer. (d) Activation of the system releases the micropillars and inserts the DMNs into the skin through the injector spring. (e) DMNs are fully inserted into the skin and immediately dissolved.

based systems also typically involve complex procedures, and require a trained professional for their administration.

In this paper, we introduce the "Microlancer", a patchless, self-administered DMN delivery system that incorporates advantages of DMN patches and needle-less jet injectors while also circumventing many of their limitations. In addition, the Microlancer is capable of inserting drug-loaded DMNs without the involvement of a patch in a minimally invasive manner.

Results

DMN array fabrication over circular holes of Microlancer system. The Microlancer is currently designed to utilize a 3 × 3 array of rounded micropillars (r = 250 μm) in order to insert DMNs into the epidermis and dermis layers of the skin (Fig. 1a). The necessary injection force is generated by thumb pressure applied along the axis of the system. In parallel, a spring also pushes the array of micropillars, in order to maintain the correct alignment of the array with respect to the skin (Supplementary Fig. S1). Upon completion of the injection, two extractor springs enable the retraction of the micropillars back into the Microlancer housing. The DMN insertion depth is completely controlled by a micropillar length alignment system. Thus, securing the correct height block inside the system controls the insertion depth of the DMNs (Fig. 1b).

In this study we utilized one of the most recently described method, called droplet-born air blowing (DAB) to fabricate DMNs[27]. Briefly, DMNs with a height of 600 μm and a tip radius of 10 μm were fabricated over a 3 × 3 array of circular holes (r = 252 μm), in order to easily and consistently enable the physical detachment of DMNs. The array of holes was then coated with a thin layer of carboxymethyl cellulose (CMC), which provides the base for the fabrication of DMNs. In addition, since the coating mixture and the polymer used in the DMNs were composed of the same material, the CMC layer was dissolved slightly after fabrication and became thinner over the holes compared to the rest of the coating. A protective layer ensures that only the DMNs, and not the surrounding base layer material, is inserted into the skin (Fig. 1c). Activation of the system restores the compressed alignment springs to their equilibrium lengths, thereby forcing the micropillars through the holes and resulting in the detachment of the DMNs and their insertion into the skin. The micropillars are then compressed and retracted back into the system (Fig. 1d). The DMN layer can be immediately replaced with a new one upon application for next injection. Since the insertion of the DMNs is assisted by micropillars, the Microlancer consistently achieves complete insertion into the skin with high efficiency (Fig. 1e). We also conducted mechanical fracture force tests to determine the maximum axial load that can be applied to DAB-fabricated DMNs without failure (Supplementary Fig. S2a). The maximum axial load was determined to be approximately 0.498 N, a force that is 8 times higher than the minimum penetration force required for DMN skin penetration (Supplementary Fig. S2b)[25,31].

Video imaging of injection process. In order to visually capture the mechanical performance of the Microlancer, the insertion of DMNs

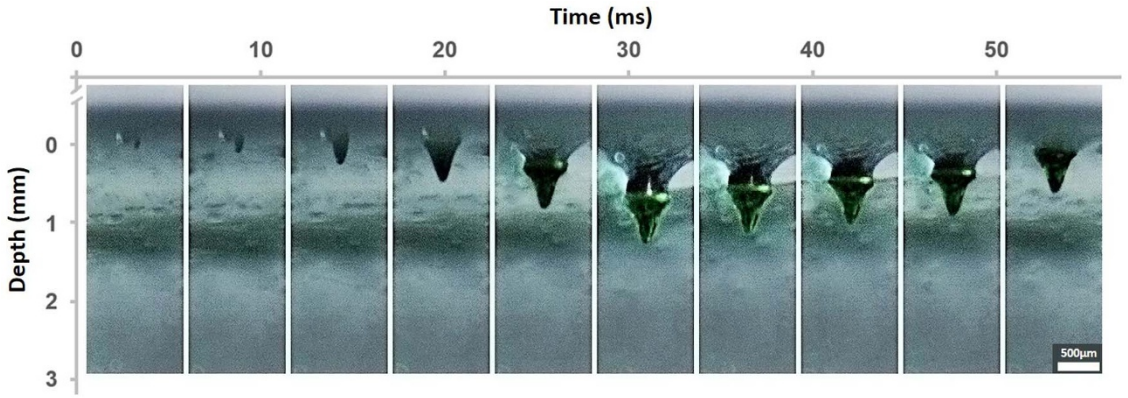

Figure 2 | DMN injection into polyacrylamide gel. Complete insertion was achieved by 0.5 s, with a depth of approximately 650 μm.

into a polyacrylamide gel was recorded using a high-speed camera. Although poly acrylamide gel does not fully mimic human skin, it is widely used due to its transparency and skin-like properties[29,32]. The position of the DMN tip was tracked using microscopic calibration software by evaluating still photographs. The minimum insertion depth (50 μm) was chosen as representative depth for controlled insertion performed by the Microlancer. The whole process lasted approximately 0.5 s (Fig. 2).

Controlled insertion depth. Histological examination was performed to verify that the targeted skin insertion depth correlated with the actual skin insertion depth. We chose 50 and 100 μm insertion depths to study the accuracy of the Microlancer. To facilitate the sectioning process, we treated the skin with 10% methylene blue dye solution. In subsequent trials, hairless pig cadaver skin was used as a mimic to human skin (Fig. 3a). DMNs (h = 600 μm) inserted 50 μm deep into hairless skin were clearly visible beneath the skin; these DMNs pierced an average distance of 650 ± 10 μm (Fig. 3b). DMNs that were inserted 100 μm into the skin were less apparent on microscopy. Histological examination indicated that these DMNs had penetrated 700 ± 20 μm into the skin (Fig. 3c). To ensure the reproducibility and accuracy of the Microlancer, regardless of skin type or the amount of hair on the skin, we performed a similar set of experiments using hairy pig cadaver skin (Fig. 3d). The DMNs that were inserted 50 μm deep into the hairy skin yielded insertion spots that were similar to the appearance of the spot array on the hairless skin, with an average insertion depth of 650 ± 10 μm (Fig. 3e). In addition, histological examinations of the DMNs inserted 100 μm deep into the hairy skin also yielded similar result to those inserted into hairless skin (Fig. 3f).

Drug release profile comparison. To compare the drug release efficiency of the Microlancer with that of the DMN patch, we set up a Franz diffusion cell for insulin-loaded DMNs. A Franz diffusion cell mimics the natural blood circulation of the body by using a body temperature stimulator receptor and a donor cell (Supplementary Fig. S3). Insulin-loaded (0.2 IU) CMC DMNs were applied to pig cadaver skin; two groups of DMNs were investigated, the DMN patch group and the Microlancer group (n = 3 per group). The sections of pig cadaver skin were then fixed and pressed with a pinch clamp over the Franz diffusion cell. Samples were taken from the receptors at 10, 20, 30, 60 and 120 min, and the amount of insulin in each sample was quantitated using an insulin ELISA kit (n = 3 per group). The insulin release profiles of the Microlancer and the DMN patch differed greatly after only 10 min. While the DMN patch had only released 12 ± 2% of its total insulin content after 10 min, the Microlancer (set at 50 μm) had already delivered 46 ± 1% ($p < 0.0001$). At 2 h post-application, the DMN patch had released 56 ± 5% of its total insulin content, whereas the Microlancer had released 92 ± 2% ($p < 0.0001$) (Fig. 4a). To analyze the insertion efficacy of the DMNs into hairy skin, we set up a Franz diffusion cell under the same conditions, except that hairy pig cadaver skin was used. Insulin release profiles were measured at the same time intervals as in the first study. The insulin release profiles of the DMNs inserted by the Microlancer remained constant, whereas the DMNs inserted by the patch had only delivered 26 ± 2% of their total insulin content after 2 h ($p = 0.0001$) (Fig. 4b). Therefore, these results indicate that, unlike the DMN patch, the Microlancer is capable of inserting DMNs into either hairy or hairless skin with the same level of efficacy.

Strikingly, even though the DMNs were inserted only 50 μm deep into the surface layer of the pig cadaver skin, the drug release achieved was approximately 92%. We hypothesized that the remaining 8% of the drugs that had failed to be released represented a small population of surface-resident drugs. Therefore, we next set the micropillars to insert DMNs 100 μm deep into both hairy and hairless skin. The drug release profile of DMNs inserted 100 μm deep reached 97 ± 2%, which was approximately 5% higher than the profile obtained with DMNs inserted 50 μm deep into the skin ($p < 0.0001$).

To further investigate drug release profile differences, we compared the physical shapes of the DMNs before and after 2 h application using bright field light microscopy. We found that the DMNs fabricated over the patch were not fully inserted into the pig cadaver skin. In the hairless skin, about one-third of the total DMNs remained intact on the patch (Fig. 4c). The portion of DMNs remained on the patch was about two-third for the hairy pig cadaver skin (Fig. 4d). Unlike the patch, the DMNs that had been fabricated over the holes in the Microlancer were completely detached from the base and were successfully inserted into the skin (Fig. 4e).

Insulin loaded DMNs biological activity test. To confirm the biological activity of insulin loaded DMNs, the biological activity of 0.2 IU insulin was measured before and after DMN fabrication, using insulin ELISA kit. The biological activity of insulin, insulin mixed with CMC solution and insulin loaded DMNs were 99 ± 1%, 97 ± 2.4% and 95 ± 3.3% respectively.

DMN encapsulated insulin stability test. To ensure the potency of the insulin delivered by the DMNs, we examined the stability of 0.2 IU of insulin both before and after encapsulation in DMNs, using ultra performance liquid chromatography (UPLC). UPLC data showed that the biological activity of insulin was successfully preserved after DMN fabrication (n = 3).

Effectiveness of insulin loaded Microlancer compared with patch and SC in diabetic mice. To examine the *in vivo* delivery efficacy of the Microlancer compared with the DMN patch and with subcutaneous (SC) injection, we measured changes in the blood glucose levels of diabetic mice after the delivery of insulin.

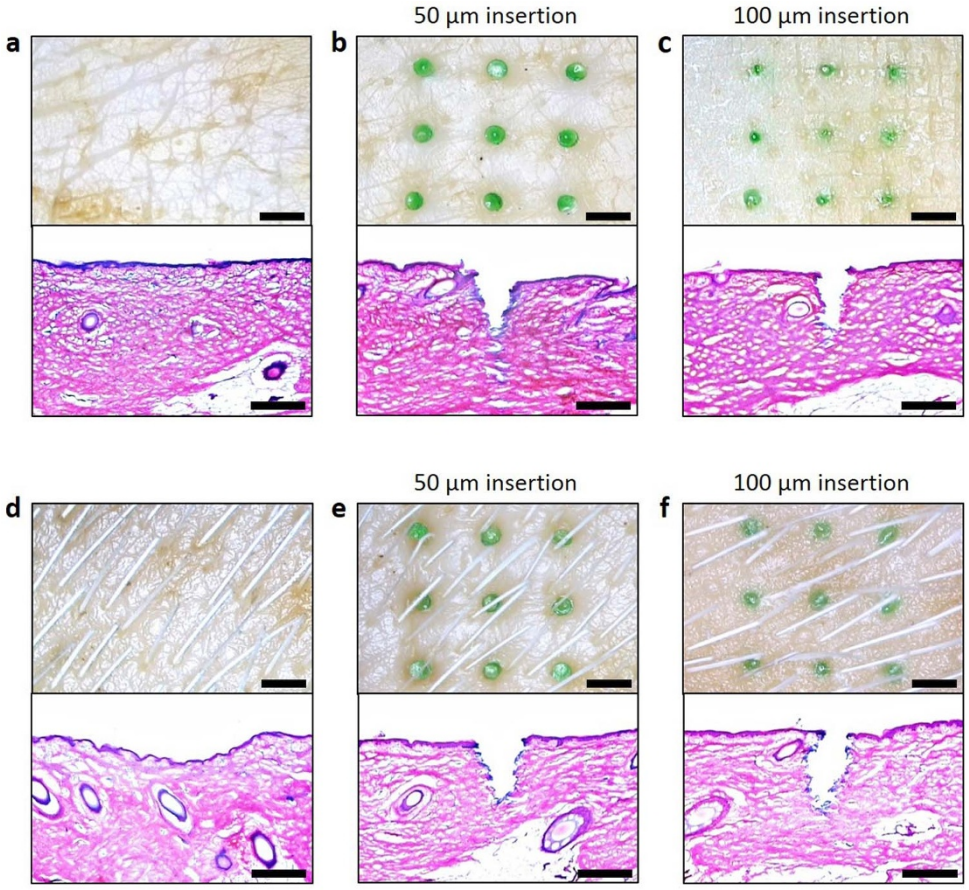

Figure 3 | Microscopy images and histological examinations of hairy and hairless pig cadaver skin. (a) Hairless pig cadaver skin before DMN insertion. (b) 50-μm insertion of 600-μm-tall DMN. The DMN was inserted 650 μm deep into the skin. (c) The base area of the DMN that was inserted 100 μm deep was less apparent on the skin surface compared with those inserted 50 μm deep. Histological examination showed that the DMNs were inserted 700 μm deep into the skin. (d) Hairy pig cadaver skin before DMN insertion. (e) The appearance of DMNs inserted 50 μm deep into hairy skin was similar to the appearance of DMNs inserted into hairless pig cadaver skin. (f) DMNs inserted 100 μm deep into the hairy pig cadaver skin penetrated 700 μm deep. Scale bars: microscopy images, 2 mm; histological images, 500 μm.

Diabetes was induced in the mice, and the mice were shaved at the area of DMN application in order to facilitate a more accurate comparison. DMN arrays containing 0.2 IU insulin were applied onto the skin of the mice, using either the patch or the Microlancer. To compare the DMN delivery efficiency of the Microlancer with that of subcutaneous injection, 0.2 IU of insulin was injected into mice subcutaneously. With the Microlancer, the DMNs were injected 50 μm deep into the skin. The DMN patch was applied over the skin of each mouse and additionally secured with adhesive tape. Unloaded DMNs were used as a negative control, and were inserted into the skin of control mice using the Microlancer. The changes in the plasma glucose levels of diabetic mice 6 h after the application of insulin by each method are shown in Fig. 5a.

To study the ability of DMNs to deliver insulin across the skin, the plasma insulin concentrations of treated mice were measured for 6 h. Plasma insulin concentrations in the SC group peaked after 1 h, whereas the apex was observed 2 h post-application for the DMN patch and Microlancer groups (Fig. 5b). The maximum plasma insulin concentration was 156 μIU/ml, 128 μIU/ml, and 61 μIU/ml for the SC, Microlancer and patch group, respectively. As expected, plasma insulin was not detected in the control group.

Additionally, FITC labeled insulin loaded DMNs were inserted into mice skin to further investigate the delivery efficacy of Microlancer (Fig. 5c) compared with patches (Fig. 5d). Insulin only DMNs showed no fluorescent signal whereas FITC labeled insulin loaded DMNs in both groups of Microlancer and patch exhibited a strong signal 30 min after application. Although the amount of loaded FITC was same in both groups, the intensity of fluorescence was measured to be approximately 59% higher for Microlancer. The signal strength was decreased 1 h post application.

Discussion

This is the first study to demonstrate that DMNs can be effectively applied without utilizing patches. Previously application of DMN patches into skin was highly limited due to incomplete insertion of DMNs. Here, we developed a quick, self-administered DMN delivery system called Microlancer which combines of the advantages of the DMN patch and the needle-less jet injector, while also providing accurate and consistent control of insertion depth. With this system, DMNs can be delivered in a more dose-effective manner compared to DMN patches. By comparing histological examinations obtained by the Microlancer with those of the current DMN patches, we found that the Microlancer exhibited great potential for enabling a more effective DMN-based drug delivery. Only 46 ± 1% of DMNs fabricated over patches were inserted into pig cadaver skin whereas this was 97 ± 2% for DMNs inserted using Microlancer. Studies on insertion depth accuracy of DMNs inserted into hairless and hairy pig cadaver skin using Microlancer demonstrated that the Microlancer offers a full insertion depth control, regardless of the skin type or the amount of hair on the skin. Therefore, we conclude that the Microlancer can perform effectively on a wide range of skin types.

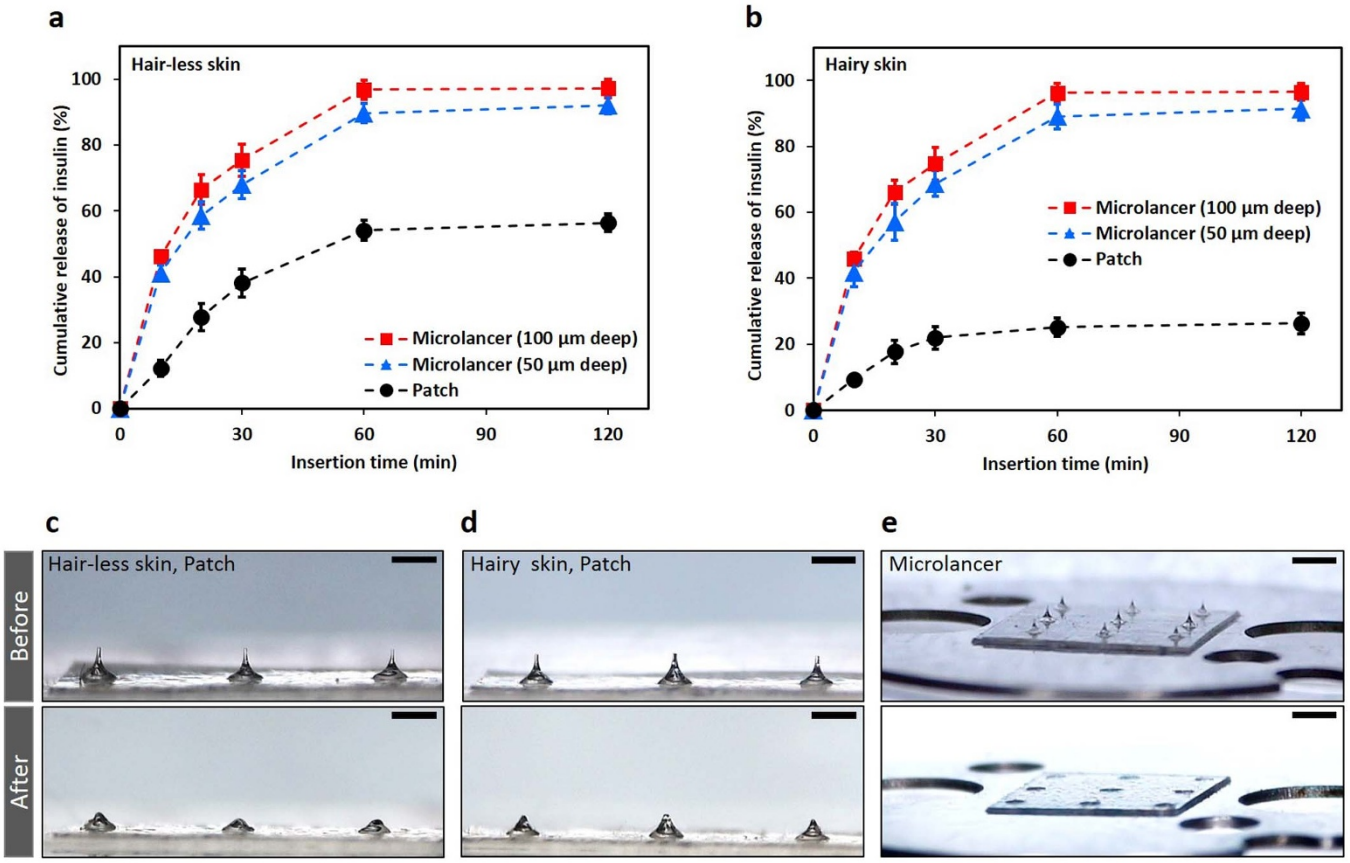

Figure 4 | Comparison of insulin release profiles obtained with the Franz diffusion cell. (a) Comparison of cumulative insulin release profiles of the DMN patch compared with the 50-µm and 100-µm insertions into sections of hairless and (b) hairy pig cadaver skin. (c) Insulin-loaded DMNs on the patch before (above) and 2 h after (below) application onto hairless and (d) hairy pig cadaver skin. (e) A 3 × 3 array of insulin-encapsulated DMNs, fabricated on the Microlancer, before (above) and after (below) application. Scale bars on (c) and (d) are 1 mm. Scale bar for (e) is 2 mm.

Our studies further revealed that in this system, although the DMNs were fully inserted, the skin was not pierced by the micropillars. This aspect of the drug delivery process is extremely important for the clinical application of the Microlancer, since it enables the painless delivery of DMNs into the skin without causing infection. Studies have shown that even when DMNs are applied at a force of 16.4 N/array, complete insertion cannot be achieved[33]. However the Microlancer is capable of performing complete DMN insertion into any skin type, regardless of the amount of hair present on the skin.

Due to rapid increase in number of patients suffering from diabetes and requirement of daily injection for these patients, we studied effectiveness of insulin DMN patches and compared those with Microlancer. The DMNs that were inserted into the diabetic mice via the Microlancer quickly lowered plasma glucose levels; moreover, the Microlancer was nearly as effective as the SC injection, which directly delivers insulin under the dermis. The blood glucose level nadir was observed approximately 1 h earlier after the SC injection compared with the Microlancer, which is likely due to the slow diffusion rate associated with the CMC DMN-encapsulated insulin. Quantitation of the plasma glucose levels showed that the DMNs fabricated over the patch were less effective in reducing the plasma glucose level compared with the Microlancer. We conclude that the lower plasma glucose levels were most likely caused by the incomplete insertion of DMNs by the patch. These findings support the difference in drug release profiles observed in the Franz diffusion cell studies between the Microlancer and the patch seen in Fig. 4. Insertion of FITC labeled insulin loaded DMNs into mice showed a 59% higher fluorescence signal intensity when applied by Microlancer compared with the patch. The higher cutaneous permeation of Microlancer additionally confirmed that DMNs fabricated over the patch had remarkably lower efficacy compared with Microlancer. In addition, this comparison revealed that the Microlancer completely inserted the insulin-loaded DMNs at a significantly faster rate, and more efficiently, compared with the DMN patches. More importantly, patients can apply the required drug dose according to their individual prescription, thus potentially improving the lives of many patients with diabetes.

Overall, the Microlancer is capable of inserting any type of drug, protein, vaccine or other biomolecules encapsulated in DMNs for a wide variety of clinical applications. We anticipate that this system will greatly impact the future of vaccine and drug delivery which should provide optimum effectiveness and patient convenience.

Methods

Fabrication of dissolving microneedles (DMNs). Humalog insulin (Eli Lilly and Company) loaded carboxymethyl cellulose (CMC, 90 KdA, Sigma-Aldrich) polymer was prepared by mixing 10% CMC powder with distilled water and then diluting insulin (0.2 IU) in phosphate-buffered saline (PBS, pH 7.4) at 37°C. The insulin-CMC solution was dispensed over the holes; holes were arranged in 3 × 3 arrays on an automated X, Y and Z stage (SHOT mini 100-s, Musashi). The solution was dispensed at a rate of 0.6 kg.f/cm and 0.05 s/aliquot. A custom-made, rate-controllable stage capable of upward and downward motion was designed in order to accurately push and pull the two smooth solid plates, which were parallel and faced each other. The insulin-loaded polymer was dispensed over the holes and placed on the lower plate of the motion stage. Another plate on top was then moved downward until it contacted the upper surface of the polymer droplets. Then, the upper stage was moved upward at rate of 3 mm/min for 17 s. The polymers were then solidified by air flow, which resulted in conical-shaped DMNs. Finally, the upper plate was drawn upward at a rate of 60 mm/min for 10 s, to separate the DMNs that had been fabricated over the holes from the upper plate. The DMNs formed over the holes were 600 µm in height, with a tip dimension of 10 ± 5 µm. The same method was used to fabricate insulin FITC

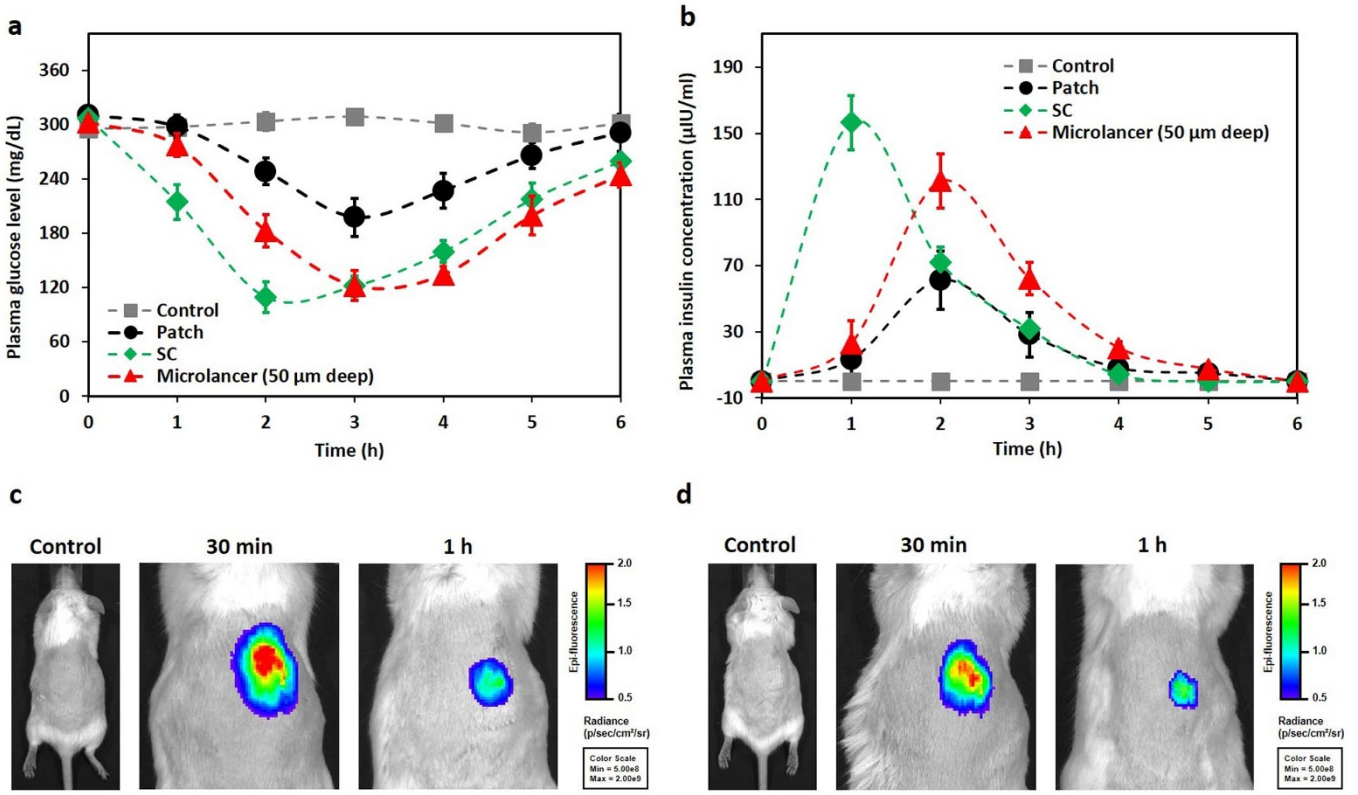

Figure 5 | ***In vivo*** **images of induced diabetic mice and the effects of insulin after its application using DMN patch, the Microlancer or subcutaneous (SC) injection.** (a) Plasma glucose level changes in diabetic mice over a period of 6 h. (b) Plasma insulin concentrations of diabetic mice in each of the groups over time. (c) Insulin labeled FITC signal intensity comparison of Microlancer and (d) patch at 30 min and 1 h post application.

labeled DMNs. Insulin loaded DMNs were fabricated as mentioned above. Next, 0.05% insulin-FITC labeled powder (Sigma-Aldrich) was added to the insulin polymer solution; the solution was mixed well for 10 min until homogeneity was reached, and then the DMNs were fabricated.

Mechanical force of a DMN. The force resulting in the mechanical failure of a single DMN was determined using a Zwick Z0.5 TN (Zwick GmbH & Co.) force analyzing machine. Briefly, a single DMN was placed on a moving sensor. Axial force was then applied at a speed of 0.05 mm/s toward a fixed rigid stainless steel stage. The force at which the tip of the DMN touched the stage and broke was measured using the Zwick Z0.5 TN acquisition software and found to be 0.498 ± 0.020 N.

Video imaging. An acrylamide gel with a viscosity of 20% was prepared by mixing distilled water with a 30% acrylamide stock and then adding 1.5 M Tris, 10% sodium dodecyl sulfate (SDS, Amresco LLC), ammonium persulfate and TEMED (Sigma-Aldrich). The gel was then allowed to polymerize at room temperature for 20 min. Using the Microlancer, DMNs were inserted into the 20% polyacrylamide gel. DMN insertion was recorded using a high-speed video camera (Phantom V710) equipped with a 200 mm micro photo lens (Nikon AF MICRO NIKKOR 200). The position of the DMN tip was carefully tracked using microscopic calibration software.

In vitro **insertion depth experiment.** Green dye loaded DMNs were employed to visualize insertion depth into both hairy and hairless pig cadaver skin using the Microlancer. The DMNs were inserted at target depths of 50 μm and 100 μm, and then stored at -10°C until analysis. The insertion depths achieved in both hairy and hairless skin were compared by microscopy and also assessed histologically. For analysis, tissue samples of the hairy and hairless pig cadaver skin with 50 μm and 100 μm insertions were embedded in OCT compound (Tissue-Tek, Sakura Finetek) at −30°C, and 25 μm sections were taken. The sections were stained with hematoxylin for 5 min and eosin for 1 min. The stained slides were then dehydrated through a series of alcohol gradients, cleared using xylene and mounted in permount (Fisher Scientific).

Insulin-loaded DMN biological activity study. The biological activity of untreated insulin, insulin mixed with CMC solution and insulin loaded DMN was measured using an insulin ELISA kit (ALPCO) according to the protocol. Insulin loaded DMNs were dissolved in PBS before measuring the biological activity.

In vitro **insulin delivery profiling.** A Franz diffusion cell (Hanson) was used to investigate the release profile in pig cadaver skin of DMNs loaded with insulin (0.2 IU). The diffusion cell was filled with 7 ml phosphate-buffered saline (PBS, pH 7.4) at room temperature, and its contents were thoroughly mixed via a magnetic stirrer (500 rpm for 15 min) before beginning the experiment. Hairy and hairless dorsal pig cadaver skins were carefully sliced into 1 × 1 × 0.2 cm pieces and placed over the filled receptor. Then, the DMN patches were inserted into the hairy and hairless cubes of pig cadaver skin, pressed by an empty donor chamber on top of the skin, and fixed with a pinch clamp (n = 3). The DMNs inserted into the hairy and hairless skin (50 μm deep) using the Microlancer were treated in the same manner (n = 3). At 10, 20, 30, 60 and 120 min post-insertion, 0.5 ml samples were taken from the receptor and insulin content was quantitated using an enzyme-linked immunosorbent assay (ELISA) kit (ALPCO). After each sample was taken, its volume was replaced with an equivalent volume of fresh buffer. All samples were stored at −10°C until analysis.

Diabetic animal model. Male C57BL/6 mice (7–8 weeks old, OrientBio) were used in this study. Mice were anesthetized with avertin (2,2,2-tribromoethanol, Sigma-Aldrich) and diabetes was then induced by an intravenous injection of streptozotocin (50 mg/kg, N-(methylnitrosocarbamoyl)-α-D-glucosamine, Sigma-Aldrich) in sodium citrate buffer (pH 4.5). All the animal studies were conducted in accordance with the Guide for the Care and Use of Laboratory Animals and performed according to procedures approved by committee of the Department of Laboratory Animal Medicine (Medical Research Center, College of Medicine, Yonsei University).

In vivo **delivery efficacy experiment.** Diabetic mice were divided into the following 4 groups: (a) an untreated group (negative control); (b) a subcutaneous injection group (0.2 IU, positive control); (c) a patch group (DMNs loaded with 0.2 IU insulin); and (d) a Microlancer group (DMNs loaded with 0.2 IU insulin) (n = 5 per group). Mice were fasted throughout the experiment, but were allowed free access to water. After the back hair was removed from each mouse using an electric shaver, 0.2 IU insulin was administered using the DMN patch, the Microlancer or a SC injection. Blood samples (0.1 ml) were collected hourly from tail-vein lacerations for 6 h post-application. Plasma was then separated by centrifuging the samples at 10,000 rpm for 15 min. The serum samples were immediately frozen at −80°C until analysis. The plasma glucose levels over time for each group were measured using a Glucose CII-Test kit. The plasma insulin concentrations were determined using an insulin ELISA kit (ALPCO).

Insulin-loaded DMN stability study. Insulin-loaded DMNs were dissolved in 1 ml of PBS (pH 7.4) and their insulin contents were quantitated using ultra-performance liquid chromatography (UPLC, ACQUITY UPLC I-Class, Waters). The UPLC

system was equipped with a TUV detector and a 2.1 × 100 mm column (Acquity, Waters). The mobile phase system consisted of (A) 0.1% trifluoroacetic acid (TFA) in DW and (B) TFA in acetonitrile (75:25 ratio). The column temperature was set to 35°C, with a flow rate of 0.250 mL/min, and compounds in the eluent were measured with a UV detector at 214 nm. A standard calibration curve was generated based on known insulin concentrations ranging from 0 IU to 1.5 IU. The areas under the curves of the insulin peaks before and after DMN fabrication were compared with one another.

Cutaneous permeation test. Insulin FITC labeled DMNs were injected into mice by Microlancer and patch. The cutaneous permeation efficacy was measured by in vivo imaging system (IVIS, Xenogen 200, Caliper life sciences) at 30 min and 1 h for 5 s each using a 150 W quartz halogen lamp, filtered at excitation wavelength of 445–490 nm and emission wavelength of 515–575 nm. All data were analyzed and expressed as photon-flux based on IVIS system software. The quantification of fluorescence intensity was measured using ImageJ software.

Statistical analysis. All experiments were performed using at least 3 samples per group and data were analyzed by analysis of variance based on GraphPad Prism software. The error bars in graphs represent standard deviation.

1. Sullivan, S. P., Murthy, N. & Prausnitz, M. R. Minimally invasive protein delivery with rapidly dissolving polymer microneedles. *Adv Mater* **20**, 933–938 (2008).
2. Prausnitz, M. R., Mitragotri, S. & Langer, R. Current status and future potential of transdermal drug delivery. *Nat Rev Drug Discov* **3**, 115–24 (2004).
3. Prausnitz, M. R. & Langer, R. Transdermal drug delivery. *Nat Biotechnol* **26**, 1261–8 (2008).
4. Pond, S. M. & Tozer, T. N. First-pass elimination. Basic concepts and clinical consequences. *Clin Pharmacokinet* **9**, 1–25 (1984).
5. Cheung, K., Han, T. & Das, D. B. Effect of Force of Microneedle Insertion on the Permeability of Insulin in Skin. *Journal of diabetes science and technology* **8**, 444–452 (2014).
6. Trim, J. C. & Elliott, T. S. A review of sharps injuries and preventative strategies. *J Hosp Infect* **53**, 237–42 (2003).
7. Nir, Y. *et al.* Fear of injections in young adults: prevalence and associations. *Am J Trop Med Hyg* **68**, 341–4 (2003).
8. Simonsen, L. *et al.* Unsafe injections in the developing world and transmission of bloodborne pathogens: a review. *Bull World Health Organ* **77**, 789–800 (1999).
9. Mohammed, Y. H. *et al.* Microneedle enhanced delivery of cosmeceutically relevant peptides in human skin. *PloS one* **9**, e101956 (2014).
10. Tuan-Mahmood, T. M. *et al.* Microneedles for intradermal and transdermal drug delivery. *Eur J Pharm Sci* **50**, 623–37 (2013).
11. Lee, K. & Jung, H. Drawing lithography for microneedles: a review of fundamentals and biomedical applications. *Biomaterials* **33**, 7309–26 (2012).
12. Zhu, Z. *et al.* Rapidly dissolvable microneedle patches for transdermal delivery of exenatide. *Pharmaceutical research* **31**, 3348–3360 (2014).
13. Kaushik, S. *et al.* Lack of pain associated with microfabricated microneedles. *Anesth Analg* **92**, 502–4 (2001).
14. Mikszta, J. A. *et al.* Improved genetic immunization via micromechanical disruption of skin-barrier function and targeted epidermal delivery. *Nat Med* **8**, 415–9 (2002).
15. Liu, S. *et al.* The development and characteristics of novel microneedle arrays fabricated from hyaluronic acid, and their application in the transdermal delivery of insulin. *J Control Release* **161**, 933–41 (2012).
16. Lee, K. *et al.* Drawing lithography: three-dimensional fabrication of an ultrahigh-aspect-ratio microneedle. *Adv Mater* **22**, 483–6 (2010).
17. Lee, J. W. *et al.* Dissolving microneedle patch for transdermal delivery of human growth hormone. *Small* **7**, 531–9 (2011).
18. Lee, K., Lee, C. Y. & Jung, H. Dissolving microneedles for transdermal drug administration prepared by stepwise controlled drawing of maltose. *Biomaterials* **32**, 3134–40 (2011).
19. Lee, J. W., Park, J. H. & Prausnitz, M. R. Dissolving microneedles for transdermal drug delivery. *Biomaterials* **29**, 2113–24 (2008).
20. Chu, L. Y. & Prausnitz, M. R. Separable arrowhead microneedles. *J Control Release* **149**, 242–9 (2011).
21. Chen, X. *et al.* Improving the reach of vaccines to low-resource regions, with a needle-free vaccine delivery device and long-term thermostabilization. *J Control Release* **152**, 349–55 (2011).
22. Van Damme, P. *et al.* Safety and efficacy of a novel microneedle device for dose sparing intradermal influenza vaccination in healthy adults. *Vaccine* **27**, 454–9 (2009).
23. van der Maaden, K., Jiskoot, W. & Bouwstra, J. Microneedle technologies for (trans)dermal drug and vaccine delivery. *J Control Release* **161**, 645–55 (2012).
24. Chen, M. C. *et al.* Fully embeddable chitosan microneedles as a sustained release depot for intradermal vaccination. *Biomatpartzzerials* **34**, 3077–86 (2013).
25. Ling, M. H. & Chen, M. C. Dissolving polymer microneedle patches for rapid and efficient transdermal delivery of insulin to diabetic rats. *Acta biomaterialia* **9**, 8952–8961 (2013).
26. Trookman, N. S., Rizer, R. L. & Weber, T. Irritation and allergy patch test analysis of topical treatments commonly used in wound care: evaluation on normal and compromised skin. *J Am Acad Dermatol* **64**, 16–22 (2011).
27. Kim, J. D. *et al.* Droplet-born air blowing: Novel dissolving microneedle fabrication. *J Control Release* **170**, 430–6 (2013).
28. Moga, K. A. *et al.* Rapidly-dissolvable microneedle patches via a highly scalable and reproducible soft lithography approach. *Adv Mater* **25**, 5060–6 (2013).
29. Taberner, A., Hogan, N. C. & Hunter, I. W. Needle-free jet injection using real-time controlled linear Lorentz-force actuators. *Med Eng Phys* **34**, 1228–35 (2012).
30. Engwerda, E. E., Tack, C. J. & de Galan, B. E. Needle-free jet injection of rapid-acting insulin improves early postprandial glucose control in patients with diabetes. *Diabetes Care* **36**, 3436–41 (2013).
31. Davis, S. P. *et al.* Insertion of microneedles into skin: measurement and prediction of insertion force and needle fracture force. *J Biomech* **37**, 1155–63 (2004).
32. Stachowiak, J. C. *et al.* Dynamic control of needle-free jet injection. *J Control Release* **135**, 104–12 (2009).
33. Donnelly, R. F. *et al.* Optical coherence tomography is a valuable tool in the study of the effects of microneedle geometry on skin penetration characteristics and in-skin dissolution. *J Control Release* **147**, 333–41 (2010).

Acknowledgments

We thank Song Her, Suyong Kim, Seolhwa Seo, Chang Yeol Lee and Huisuk Yang for their assistance with the research.

Author contributions

S.F.L. developed the Microlancer and carried out *in vivo* experiments. M.D. performed Franz diffusion cell and ELISA analysis. H.J. designed the experiments, analyzed data and wrote the manuscript.

Additional information

Supplementary information accompanies this paper at http://www.nature.com/scientificreports

Competing financial interests: The authors declare no competing financial interests.

How to cite this article: Lahiji, S.F., Dangol, M. & Jung, H. A patchless dissolving microneedle delivery system enabling rapid and efficient transdermal drug delivery. *Sci. Rep.* 5, 7914; DOI:10.1038/srep07914 (2015).

This work is licensed under a Creative Commons Attribution-NonCommercial-NoDerivs 4.0 International License. The images or other third party material in this article are included in the article's Creative Commons license, unless indicated otherwise in the credit line; if the material is not included under the Creative Commons license, users will need to obtain permission from the license holder in order to reproduce the material. To view a copy of this license, visit http://creativecommons.org/licenses/by-nc-nd/4.0/